 CMES, vol.93, no.5, pp.317-333, 2013

Thermocapillary Motion of a Spherical Drop in a Spherical Cavity

Tai C. Lee[1], **Huan J. Keh**[2]

Abstract: A theoretical study of the thermocapillary migration of a fluid sphere located at an arbitrary position inside a spherical cavity is presented in the quasi-steady limit of small Reynolds and Marangoni numbers. The applied temperature gradient is perpendicular to the line through the drop and cavity centers. The general solutions to the energy and momentum equations governing the system are constructed from the superposition of their fundamental solutions in the spherical coordinates originating from the two centers, and the boundary conditions are satisfied by a multipole collocation method. Results for the thermocapillary migration velocity of the drop are obtained for various cases. When the fluid sphere is at the center of the cavity, the collocation result is in excellent agreement with the available exact solution. The normalized thermocapillary migration velocity decreases with increases in the drop-to-cavity radius ratio and in the relative distance between the drop and cavity centers, vanishing as the drop surface touches the cavity wall. For a given configuration, this velocity augments with increases in the relative viscosity of the drop and thermal conductivity of the cavity phase. The boundary effects on the thermocapillary motion perpendicular to the line connecting the drop and cavity centers is significant, but in general weaker than that parallel to this line.

Keywords: Thermocapillary motion, Creeping flow, Spherical drop and bubble, Spherical cavity, Boundary effect.

1 Introduction

When a small drop of one fluid is suspended in a second, immiscible fluid possessing a temperature gradient, it will move in the direction of the gradient. This movement, known as thermocapillary migration and found in many practical applications

[1] Department of Chemical Engineering, National Taiwan University, Taipei 10617, Taiwan, Republic of China.

[2] Corresponding Author. Department of Chemical Engineering, National Taiwan University, Taipei 10617, Taiwan, Republic of China.
E-mail: huan@ntu.edu.tw

[Subramanian and Balasubramaniam (2001)], is caused by the temperature-induced interfacial tension gradient along the drop surface, which drags the fluids and propels the drop toward the side where its interfacial tension is low. The thermocapillary motion of drops was first demonstrated experimentally by Young, Goldstein, and Block (1959). They also obtained an analytical formula for the migration velocity $\mathbf{U}_0$ of a spherical drop of radius a placed in an unbounded fluid of viscosity η with a uniformly prescribed temperature gradient ∇T_∞ at vanishing Reynolds and Peclet (Marangoni) numbers,

$$\mathbf{U}_0 = \frac{2}{(2+k^*)(2+3\eta^*)}\left(-\frac{\partial\gamma}{\partial T}\right)\frac{a}{\eta}\nabla T_\infty, \tag{1}$$

where k^* and η^* are the ratios of thermal conductivities and viscosities, respectively, between the internal and surrounding fluids and $\partial\gamma/\partial T$ is the variation of the interfacial tension γ at the drop surface with respect to the local temperature T. The thermocapillary mobility of a spherical gas bubble (with negligible thermal conductivity and viscosity relative to the ambient liquid) is given by Eq. (1) taking $k^* = \eta^* = 0$.

In most practical applications of thermocapillary migration, fluid drops are not isolated and the surrounding fluid is externally bounded [Keh and Chen (1993); Kasumi et al. (2000); Selva, Cantat and Jullien (2011); Nguyen and Chen (2011); Yin et al. (2011); Katz et al. (2012)]. Thus, it is important to determine if the presence of neighboring boundaries significantly affects the movement of drops. Through the use of spherical bipolar coordinates, a method of reflections, and a lubrication theory, semi-analytical and asymptotic solutions for the thermocapillary migration velocity of a spherical drop in the vicinity of a planar boundary have been obtained in two principal cases: the migration perpendicular to a plane surface of constant temperature [Meyyappan, Wilcox, Subramanian (1981); Barton and Subramanian (1990); Chen and Keh (1990); Loewenberg and Davis (1993)] and the migration parallel to a plane wall prescribed with a linear temperature distribution [Meyyappan and Subramanian (1987)]. The boundary effects on thermocapillary migration were also studied analytically or semi-analytically for a fluid sphere located at an axial position in a circular tube [Chen, Dagan, Maldarelli (1991)] and at an arbitrary position between two parallel plane walls [Keh, Chen, and Chen (2002); Chang and Keh (2006)]. An important result of these investigations is that the boundary effects on thermocapillary migration are weaker than on sedimentation or buoyant rising of the drop.

The system of a spherical drop moving within a spherical cavity can be an idealized model for the drop migration in media or microchannels composed of connecting spherical pores. Recently, the thermocapillary migration of a fluid sphere in another

fluid within a spherical cavity parallel to the line connecting their centers was investigated with the use of a combined analytical-numerical method with a boundary collocation technique, and numerical results for the drop mobility were obtained [Lee and Keh (2013)]. The object of this article is to obtain a solution for the complementary thermocapillary migration of a fluid sphere inside a spherical cavity perpendicular to the line of their centers. The thermal and hydrodynamic equations governing the system are solved by using the boundary collocation method, and the wall-corrected thermocapillary mobility of the drop is obtained with good convergence. Because the governing equations for the general problem of thermocapillary migration of a drop within a cavity in an arbitrary direction are linear, its solution can be obtained as a vectorial addition of the solutions for its two subproblems: motion along the line connecting the drop and cavity centers, which was dealt with previously, and motion perpendicular to this line, which is managed in the current work.

2 Analysis

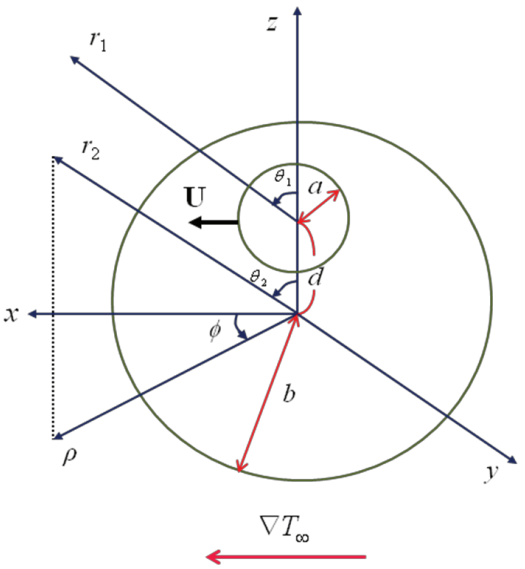

Figure 1: Geometrical sketch for the thermocapillary motion of a spherical drop in a spherical cavity perpendicular to the line connecting their centers.

We consider the quasi-steady thermocapillary migration of a spherical fluid drop of radius a in another fluid inside a spherical cavity of radius b, as shown in Fig. 1, in

which (x,y,z), (ρ,ϕ,z), and (r_2,θ_2,ϕ) are the rectangular, circular cylindrical, and spherical coordinate systems, respectively, with the origin at the center of the cavity, and (r_1,θ_1,ϕ) represent the spherical coordinates originating from the center of the drop located away from the cavity center in the z direction at a distance d. A linear temperature distribution $T_\infty(x)$ with a constant gradient $E_\infty \mathbf{e}_x$ (equal to ∇T_∞ and perpendicular to the line through the drop and cavity centers) is prescribed in the cavity surroundings far from the drop, where $\mathbf{e}_x$ is the unit vector in the x direction. To determine the thermocapillary migration velocity of the drop within the cavity, the temperature and fluid velocity fields need to be found first.

2.1 Temperature distributions

For the heat transfer in a system of thermocapillary migration, the Marangoni number can be assumed to be small. Hence, the equations of energy governing the temperature distributions are the Laplace equations

$$\nabla^2 \hat{T} = 0 \tag{2}$$

for the fluid drop ($r_1 \le a$),

$$\nabla^2 T = 0 \tag{3}$$

for the external fluid ($r_1 \ge a$ and $r_2 \le b$), and

$$\nabla^2 T_w = 0 \tag{4}$$

for the cavity surroundings ($r_2 \ge b$).

The boundary conditions require that the temperature and the normal component of heat flux be continuous at the drop surface and cavity wall as well as that the temperature field in the cavity phase far away from the drop approach the undisturbed values. Thus,

$$r_1 = a: \quad T = \hat{T}, \tag{5}$$

$$k\frac{\partial T}{\partial r_1} = \hat{k}\frac{\partial \hat{T}}{\partial r_1}, \tag{6}$$

$$r_2 = b: \quad T = T_w, \tag{7}$$

$$k\frac{\partial T}{\partial r_2} = k_w\frac{\partial T_w}{\partial r_2}, \tag{8}$$

$$r_2 \to \infty: \quad T_w \to T_\infty = T_0 + E_\infty x, \tag{9}$$

where k, $\hat{k}$, and k_w denote the constant thermal conductivities of the external fluid, the drop phase, and the cavity surroundings, respectively, and T_0 is the temperature at the center of the cavity.

The general solution of the temperature distributions can be expressed as

$$\hat{T} = T_0 + E_\infty \sum_{n=1}^{\infty} R_{1n} r_1^n P_n^1(\mu_1)\cos\phi, \tag{10}$$

$$T = T_0 + E_\infty \sum_{n=1}^{\infty} [S_{1n} r_1^{-n-1} P_n^1(\mu_1) + R_{2n} r_2^n P_n^1(\mu_2)]\cos\phi, \tag{11}$$

$$T_w = T_0 + E_\infty x + E_\infty \sum_{n=1}^{\infty} S_{2n} r_2^{-n-1} P_n^1(\mu_2)\cos\phi, \tag{12}$$

where P_n^1 is the associated Legendre function of the first kind of order n and degree one and μ_i is used to denote $\cos\theta_i$ for brevity. Equations (10)-(12) satisfies Eq. (9) and the constraint of finite temperature in the fluid phases immediately, and R_{in} and S_{in} with $i = 1$ and 2 are unknown coefficients to be determined using the boundary conditions at the drop and cavity surfaces. In the construction of the solution in Eq. (11), the general solutions to the Laplace Eq. (3) in two different spherical coordinates are superimposed. The solutions in Eqs. (10)-(12) contain only terms of $\cos\phi$ and $\sin\phi$ (no higher-order harmonics) due to the axial symmetry of the sphere-in-sphere geometry.

Substituting Eqs. (10)-(12) into Eqs. (5)-(8), we obtain

$$\sum_{n=1}^{\infty} \{(S_{1n} a^{-n-1} - R_{1n} a^n) P_n^1(\mu_1) + R_{2n}[r_2^n P_n^1(\mu_2)]_{r_1=a}\} = 0, \tag{13}$$

$$\sum_{n=1}^{\infty} \{[(n+1) S_{1n} a^{-n-2} + n k^* R_{1n} a^{n-1}] P_n^1(\mu_1) - R_{2n}[\delta_n^{(1)}(\rho, z)]_{r_1=a}\} = 0, \tag{14}$$

$$\sum_{n=1}^{\infty} \{S_{1n}[r_1^{-n-1} P_n^1(\mu_1)]_{r_2=b} + (R_{2n} b^n - S_{2n} b^{-n-1}) P_n^1(\mu_2)\} = b(1-\mu_2^2)^{1/2}, \tag{15}$$

$$\sum_{n=1}^{\infty} \{k_w^* S_{1n}[\delta_n^{(2)}(\rho, z)]_{r_2=b} + [n k_w^* R_{2n} b^{n-1} + (n+1) S_{2n} b^{-n-2}] P_n^1(\mu_2)\} = (1-\mu_2^2)^{1/2}, \tag{16}$$

where $k^* = \hat{k}/k$, $k_w^* = k/k_w$, and the functions $\delta_n^{(1)}$ and $\delta_n^{(2)}$ are defined by Eqs. (A1) and (A2) in Appendix A.

Examination of Eqs. (13)-(16) indicates that the solution of the coefficient matrix is independent of the ϕ coordinate of the boundary points on the spherical surfaces $r_1 = a$ and $r_2 = b$. A multipole collocation method [Keh and Chang (2010); Wan and Keh (2011)] to truncate the infinite series in Eqs. (10)-(12) after M terms and to enforce the boundary conditions in Eqs. (13)-(16) at M discrete points on each longitudinal arc of the drop and cavity surfaces (with values of θ_i between 0 and π) leads to a system of $4M$ simultaneous linear algebraic equations. This matrix equation can be numerically solved to yield the $4M$ unknown constants R_{in} and S_{in} appearing in the truncated form of Eqs. (10)-(12). The temperature field is completely obtained once these constants are solved for a sufficiently large value of M.

2.2 Fluid velocity distributions

Having obtained the solution for the temperature distribution on the drop surface which drives the thermocapillary migration, we can now proceed to find the velocity field. Owing to the low Reynolds number encountered in thermocapillary motions, the fluid motion is governed by the Stokes equations,

$$\hat{\eta}\nabla^2\hat{\mathbf{v}} - \nabla\hat{p} = \mathbf{0}, \tag{17}$$

$$\nabla\cdot\hat{\mathbf{v}} = 0, \tag{18}$$

$$\eta\nabla^2\mathbf{v} - \nabla p = \mathbf{0}, \tag{19}$$

$$\nabla\cdot\mathbf{v} = 0, \tag{20}$$

where $\hat{\mathbf{v}}$ and $\mathbf{v}$ are the fluid velocities for the flow in the drop ($r_1 \le a$) and for the external flow ($r_1 \ge a$ and $r_2 \le b$), respectively, $\hat{p}$ and p are the corresponding pressure distributions, and $\hat{\eta}$and η are the corresponding viscosities.

The boundary conditions for the fluid velocities at the drop surface [Young, Goldstein, and Block (1959); Anderson (1985)] and cavity wall are

$$r_1 = a: \quad (\mathbf{I}-\mathbf{e}_{r1}\mathbf{e}_{r1})\mathbf{e}_{r1}:(\boldsymbol{\tau}-\hat{\boldsymbol{\tau}}) = -\frac{\partial\gamma}{\partial T}(\mathbf{I}-\mathbf{e}_{r1}\mathbf{e}_{r1})\cdot\nabla T, \tag{21}$$

$$\mathbf{v} = \hat{\mathbf{v}}, \tag{22}$$

$$\mathbf{e}_{r1}\cdot(\mathbf{v}-U\mathbf{e}_x) = 0, \tag{23}$$

$$r_2 = b: \quad \mathbf{v} = \mathbf{0}. \tag{24}$$

Here, $\boldsymbol{\tau} = \eta[\nabla\mathbf{v} + (\nabla\mathbf{v})^T]$ and $\hat{\boldsymbol{\tau}} = \hat{\eta}[\nabla\hat{\mathbf{v}} + (\nabla\hat{\mathbf{v}})^T]$ are the viscous stress tensors, $\mathbf{e}_{ri}$ are the radial unit vectors in the two spherical coordinate systems, I is the unit dyadic, ∇T can be evaluated from the temperature distribution given by Eq. (11)

with constants obtained from Eqs. (13)-(16), and U is the thermocapillary migration velocity of the drop to be determined.

The general solution of the fluid velocity distributions satisfying Eqs. (17)-(20) in spherical coordinates of the two different origins was given by Eqs. (6)-(11) in Lee and Keh (2012). Applying the boundary conditions at the drop and cavity surfaces given by Eqs. (21)-(24) together with Eq. (11) to this general solution, we obtain

$$\begin{aligned}
&\sum_{n=1}^{\infty}[B_{1n}B_{1n}^{*}+C_{1n}C_{1n}^{*}+A_{1n}A_{1n}^{*}+B_{2n}B_{2n}^{*}+C_{2n}C_{2n}^{*}+A_{2n}A_{2n}^{*}]_{r_1=a}\\
&+\eta^{*}\sum_{n=1}^{\infty}\{2[\hat{C}_n(n-1)a^{n-2}\\
&+\hat{A}_n\frac{n(n+2)}{n+1}a^{n}]\frac{\mathrm{d}P_n^1(\mu_1)}{\mathrm{d}\mu_1}(1-\mu_1^2)^{1/2}-\hat{B}_n(n-1)a^{n-1}P_n^1(\mu_1)(1-\mu_1^2)^{-1/2}\}\\
&=-(\frac{\partial\gamma}{\partial T})\frac{E_\infty}{\eta}\sum_{n=1}^{\infty}\{S_{1n}\delta_n^{(3)}(a,\theta_1)+R_{2n}[\delta_n^{(4)}(\rho,z)]_{r_1=a}\},
\end{aligned}\tag{25}$$

$$\begin{aligned}
&\sum_{n=1}^{\infty}[B_{1n}B_{1n}^{**}+C_{1n}C_{1n}^{**}+A_{1n}A_{1n}^{**}+B_{2n}B_{2n}^{**}+C_{2n}C_{2n}^{**}+A_{2n}A_{2n}^{**}]_{r_1=a}\\
&+\eta^{*}\sum_{n=1}^{\infty}\{2[\hat{C}_n(n-1)a^{n-2}\\
&+\hat{A}_n\frac{n(n+2)}{n+1}a^{n}]P_n^1(\mu_1)(1-\mu_1^2)^{-1/2}-\hat{B}_n(n-1)a^{n-1}\frac{\mathrm{d}P_n^1(\mu_1)}{\mathrm{d}\mu_1}(1-\mu_1^2)^{1/2}]\}\\
&=-(\frac{\partial\gamma}{\partial T})\frac{E_\infty}{\eta}\sum_{n=1}^{\infty}\{S_{1n}\delta_n^{(5)}(a,\theta_1)+R_{2n}[\delta_n^{(6)}(\rho,z)]_{r_1=a}\},
\end{aligned}\tag{26}$$

as well as Eqs. (15a-d) and (16) in Lee and Keh (2012). In Eqs. (25) and (26), $\eta^{*}=\hat{\eta}/\eta$, the functions $\delta_n^{(3)}$, $\delta_n^{(4)}$, $\delta_n^{(5)}$, and $\delta_n^{(6)}$ are defined by Eqs. (A3)-(A6), the starred A_{in}, B_{in}, and C_{in} with $i=1$ and 2 are functions of position given by Eqs. (A1)-(A12) in Lee and Keh (2012), the first M coefficients S_{1n} and R_{2n} can be obtained through the procedure given in the previous subsection, and A_{in}, B_{in}, C_{in}, $\hat{A}_n$, $\hat{B}_n$, and $\hat{C}_n$ are the unknown constants in the general solution of the fluid velocity distributions to be determined.

Equations (25) and (26) together with Eqs. (15a-d) and (16) in Lee and Keh (2012) can also be satisfied by utilizing the collocation method, which is independent of the ϕ coordinate of the boundary points on the drop and cavity surfaces. Along the longitudinal arc at each spherical surface, these equations are applied at N discrete points (from $\theta_i=0$ to $\theta_i=\pi$) and their infinite series are truncated after N terms. This generates a set of $9N$ linear algebraic equations for the $9N$ unknown constants

A_{in}, B_{in}, C_{in}, $\hat{A}_n$, $\hat{B}_n$, and $\hat{C}_n$. Once these constants are solved for a sufficiently large number of N, the fluid velocity distributions are obtained completely.

2.3 Drop velocity

The drag force acting on the drop by the ambient fluid can be determined from

$$\mathrm{F} = 8\pi\eta A_{11}, \tag{27}$$

where only the lowest constant A_{11} makes a contribution. Since the drop is freely suspended in the surrounding fluid, the net force on it must vanish and Eq. (27) leads to

$$A_{11} = 0. \tag{28}$$

To determine the thermocapillary migration velocity U of the drop, Eq. (28) and the $9N$ algebraic equations need to be solved simultaneously.

3 Results and discussion

The solution for the thermocapillary migration of a fluid sphere inside a spherical cavity perpendicular to the line of the drop and cavity centers, obtained by using the boundary collocation technique described in the previous section, is presented in this section. The details of this collocation scheme are given by Lee and Keh (2012) for the creeping motion of a drop in a cavity with the same geometry but driven by a body force, in which very good accuracy and convergence behavior were achieved.

Numerical solutions for the thermocapillary migration velocity of the confined spherical drop are presented in Table 1 and Figs. 2-4 for the case of $k_w^* = k/k_w = 1$ and various values of the drop-to-cavity radius ratio a/b, relative distance between the centers of the drop and cavity $d/(b-a)$, and relative drop viscosity η^*. The corresponding velocity of a fluid sphere in an unbounded fluid, U_0 given by Eq. (1), is used to normalize the boundary-corrected values. All results in the table converge to at least the figures as shown. The temperature distributions in a bounded system with $k_w^* = 1$ are identical to those in the corresponding unbounded system, and thus the normalized thermocapillary migration velocity U/U_0 of the drop is independent of its relative thermal conductivity k^*. For any values of k^* and η^*, the drop migrates with the velocity that would exist in the absence of the cavity wall ($U/U_0 = 1$) as $k_w^* = 1$ and $a/(b-d) = 0$ (the wall is infinitely far from the drop).

For the particular case of a spherical drop situated at the center of a spherical cavity, the exact solution of its thermocapillary migration velocity was obtained explicitly as [Lee and Keh (2013)]

Table 1: The normalized thermocapillary mobility U/U_0 of a spherical drop in a spherical cavity with $k_w^* = 1$ at various values of a/b, $d/(b-a)$, and η^*.

$d/(b-a)$	a/b	U/U_0			
		$\eta^* = 0$	$\eta^* = 1$	$\eta^* = 10$	$\eta^* \to \infty$
0.25	0.1	0.99724	0.99726	0.99727	0.99740
	0.2	0.97832	0.97888	0.97920	0.97935
	0.3	0.92832	0.93221	0.93439	0.93491
	0.4	0.83459	0.84883	0.85698	0.85867
	0.5	0.69088	0.72588	0.74702	0.75122
	0.6	0.50524	0.56758	0.60970	0.61825
	0.7	0.30646	0.38676	0.45339	0.46833
	0.8	0.13733	0.20646	0.28782	0.31048
	0.9	0.03243	0.06147	0.12381	0.15236
	0.95	0.00766	0.01672	0.04864	0.07513
	0.975	0.00187	0.00436	0.01711	0.03735
	0.99	0.00029	0.00071	0.00363	0.01483
0.5	0.1	0.99601	0.99606	0.99609	0.99646
	0.2	0.97122	0.97227	0.97283	0.97324
	0.3	0.91105	0.91712	0.92040	0.92124
	0.4	0.80564	0.82500	0.83587	0.83813
	0.5	0.65341	0.69601	0.72177	0.72638
	0.6	0.46749	0.53669	0.58440	0.59413
	0.7	0.27810	0.36062	0.43182	0.44773
	0.8	0.12305	0.18989	0.27268	0.29625
	0.9	0.02894	0.05580	0.11643	0.14541
	0.95	0.00690	0.01508	0.04531	0.07179
	0.975	0.00167	0.00390	0.01576	0.03560
	0.99	0.00026	0.00064	0.00331	0.01417

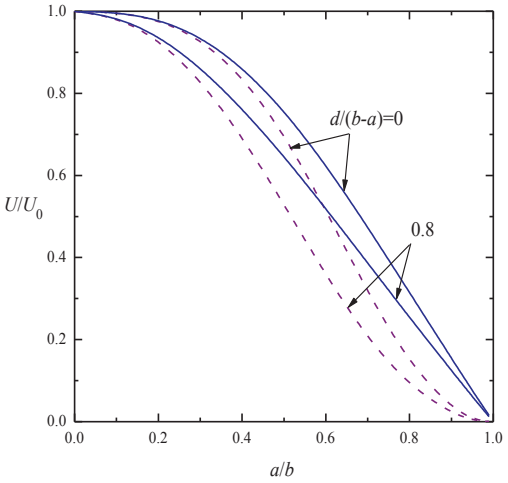

Figure 2: Plots of the normalized thermocapillary mobility U/U_0 of a drop in a cavity with $k_w^* = 1$ versus the radius ratio a/b with $d/(b-a)$ as a parameter. The solid and dashed curves denote the cases of $\eta^* \to \infty$ and $\eta^* = 0$, respectively.

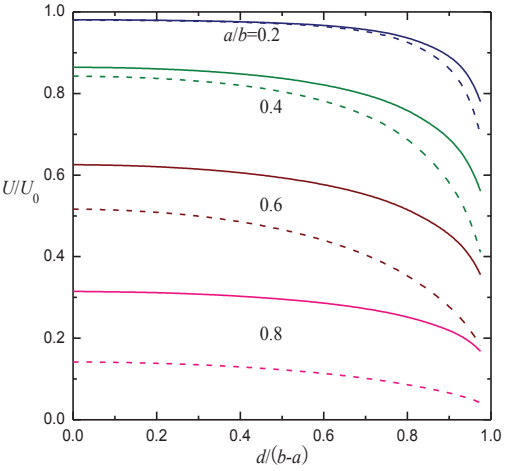

Figure 3: Plots of the normalized thermocapillary mobility U/U_0 of a drop in a cavity with $k_w^* = 1$ versus the normalized center-to-center distance $d/(b-a)$ with a/b as a parameter. The solid and dashed curves denote the cases of $\eta^* \to \infty$ and $\eta^* = 0$, respectively.

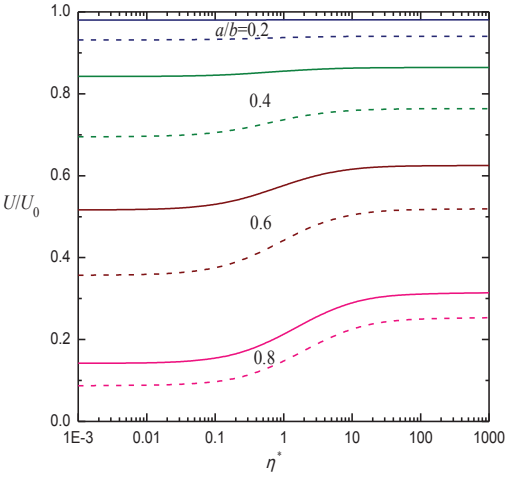

Figure 4: Plots of the normalized thermocapillary mobility U/U_0 of a drop in a cavity with $k_w^* = 1$ versus the viscosity ratio η^* with a/b as a parameter. The solid and dashed curves denote the cases of $d/(b-a) = 0$ and $d/(b-a) = 0.8$, respectively.

$$\frac{U}{U_0} = \frac{3}{2}(2+k^*)(2+3\eta^*)(1-\lambda)^2(2+4\lambda+6\lambda^2+3\lambda^3) \times [2+3\eta^*+3(1-\eta^*)\lambda^5]^{-1}[(2+k^*)(2+k_w^*)+2(1-k^*)(1-k_w^*)\lambda^3]^{-1}, \tag{29}$$

where $\lambda = a/b$. Our numerical results of U/U_0 for the concentric case of $d/(b-a) = 0$ shown in Figs. 2-4 are in excellent agreement with this exact solution.

The numerical results in Table 1 and Figs. 2-4 for the case of $k_w^* = 1$ indicate that the boundary effect on the thermocapillary migration is significant and U/U_0 decreases monotonically with an increase in the radius ratio a/b from unity at $a/b = 0$ to zero at $a/b = 1$, keeping the values of η^* and $d/(b-a)$ unchanged. For constant values of η^* and a/b, U/U_0 also decreases monotonically with an increase in $d/(b-a)$ and vanishes in the touching limit of the two surfaces $[d/(b-a) = 1]$. For fixed values of a/b and $d/(b-a)$, U/U_0 increases monotonically with an increase in η^*, opposite to that for the motion of a drop in a cavity driven by a body-force field, where the wall retardation effect on the drop mobility in general becomes stronger when the value of η^* is larger for a given configuration. Figure 4 shows that, beyond the range of $0.1 < \eta^* < 10$, U/U_0 is not a sensitive function of η^*.

The numerical solutions for the normalized thermocapillary migration velocity $U/$

U_0 of a spherical gas bubble (with $k^* = \eta^* = 0$) inside a spherical cavity perpendicular to the line connecting their centers are presented in Table 2 and Fig. 5 for various values of the parameters k_w^*, a/b, and $d/(b-a)$. Again, U/U_0 decreases monotonically with increases in a/b and $d/(b-a)$, keeping the other factors unchanged, and vanishes in the limit of touching surfaces [$d/(b-a) = 1$]. For the case of $k_w^* \neq 1$, U/U_0 no longer equals unity as $a/(b-d) = 0$ (which also implies that $a/b = 0$). For given values of a/b and $d/(b-a)$, U/U_0 decreases monotonically with an increase in k_w^* from a saturation state at $k_w^* = 0$ to zero as $k_w^* \to \infty$. This trend also occurs for the thermocapillary migration of a liquid drop.

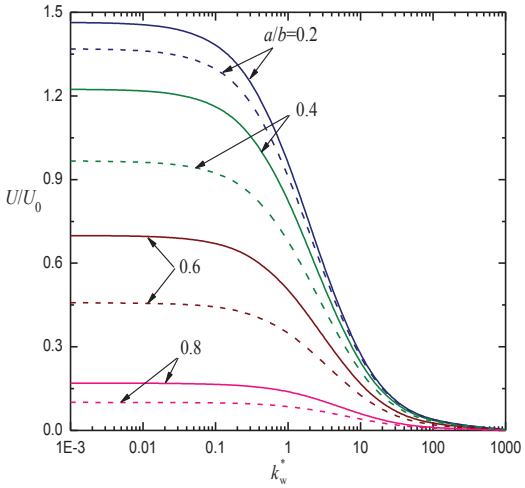

Figure 5: Plots of the normalized thermocapillary mobility U/U_0 of a gas bubble (with $k^* = \eta^* = 0$) in a cavity versus the thermal conductivity ratio k_w^* with a/b as a parameter. The solid and dashed curves denote the cases of $d/(b-a) = 0$ and $d/(b-a) = 0.8$, respectively.

The results for the normalized thermocapillary mobility U/U_0 of a confined fluid sphere with $\eta^* = 1$ and $a/b = 0.5$ are plotted versus the thermal conductivity ratio k^* in Fig. 6 for various values of the parameters k_w^* and $d/(b-a)$. Again, U/U_0 decreases monotonically with increases in k_w^* and $d/(b-a)$, keeping the other factors unchanged. On the other hand, U/U_0 increases with an increase in k^* for the case of $k_w^* < 1$, decreases with an increase in k^* for the case of $k_w^* > 1$, and is independent of k^* for the case of $k_w^* = 1$.

The governing equations for the general problem of thermocapillary migration of a fluid sphere within a spherical cavity in an arbitrary direction are linear. Therefore,

Table 2: The normalized thermocapillary mobility U/U_0 of a gas bubble (with $k^* = \eta^* = 0$) in a spherical cavity at various values of a/b, $d/(b-a)$, and k_w^*.

$d/(b-a)$	a/b	U/U_0			
		$k_w^* = 0$	$k_w^* = 0.5$	$k_w^* = 2$	$k_w^* = 10$
0.25	0.1	1.49498	1.19641	0.74814	0.24952
	0.2	1.46086	1.17187	0.73537	0.24621
	0.3	1.37207	1.10743	0.70138	0.23727
	0.4	1.21018	0.98795	0.63681	0.21984
	0.5	0.97213	0.80778	0.53572	0.19148
	0.6	0.68136	0.58028	0.40137	0.15169
	0.7	0.39092	0.34360	0.25196	0.10395
	0.8	0.16352	0.14929	0.11836	0.05621
	0.9	0.03559	0.03394	0.02979	0.01802
	0.95	0.00809	0.00790	0.00737	0.00543
	0.975	0.00192	0.00190	0.00183	0.00154
	0.99	0.00030	0.00030	0.00029	0.00027
0.5	0.1	1.49254	1.19475	0.74735	0.24933
	0.2	1.44698	1.16240	0.73073	0.24505
	0.3	1.33932	1.08464	0.68994	0.23435
	0.4	1.15787	0.95044	0.61718	0.21464
	0.5	0.90871	0.76046	0.50952	0.18416
	0.6	0.62229	0.53407	0.37395	0.14347
	0.7	0.35039	0.31015	0.23034	0.09684
	0.8	0.14509	0.13318	0.10677	0.05180
	0.9	0.03159	0.03021	0.02670	0.01649
	0.95	0.00721	0.00705	0.00661	0.00494
	0.975	0.00171	0.00169	0.00163	0.00139
	0.99	0.00027	0.00026	0.00026	0.00024

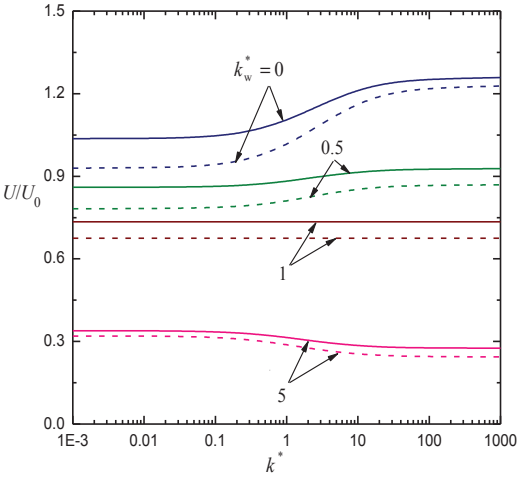

Figure 6: Plots of the normalized thermocapillary mobility U/U_0 of a drop in a cavity with $a/b = 0.5$ and $\eta^* = 1$ versus the thermal conductivity ratio k^* with k_w^* as a parameter. The solid and dashed curves denote the cases of $d/(b-a) = 0$ and $d/(b-a) = 0.6$, respectively.

its net solution can be obtained as a simple superposition of the solutions for its two subproblems: migration normal to the line connecting the drop and cavity centers, which is investigated herein, and migration parallel to this line, whose numerical solutions for the drop velocity were obtained by Lee and Keh (2013). A comparison between the results of both subproblems shows that the cavity wall in general affects the most (results in the smallest U/U_0) for the drop when its migration is parallel to the line of centers, and the least when the migration is perpendicular to it, but their difference is not significant and there exist exceptions for the case of $\eta^* \to 0$ and a/b is moderately small. Consequently, the direction of thermocapillary migration of a spherical drop inside a spherical cavity is different from that of the imposed temperature gradient, unless it is parallel or perpendicular to the line of centers.

4 Concluding remarks

In this paper, the quasi-steady thermocapillary migration of a spherical fluid drop at an arbitrary position within a spherical cavity perpendicular to the line connecting their centers in the limit of vanishing Marangoni and Reynolds numbers has been investigated by using the boundary collocation method. Numerical solutions for

the drop velocity are obtained for various values of the drop-to-cavity radius ratio, relative distance between the drop and cavity centers, and relative thermal and hydrodynamic properties of the fluid and cavity phases. These results agree excellently with the available analytical solution given by Eq. (29) for the special case of a drop located at the center of a cavity. The boundary effect on the thermocapillary migration of a drop in a cavity can be significant in appropriate situations. For the migration of a spherical drop within a spherical cavity perpendicular to the line through their centers driven by a body-force, the numerical solutions of the drop mobility were obtained by Lee and Keh (2012). A comparison of these solutions with the present results shows that the wall effect on the thermocapillary migration of a drop is weaker than that on a settling or buoyantly rising drop.

The mobility of a spherical drop undergoing thermocapillary migration in a second fluid within a spherical cavity along the line of their centers was determined by Lee and Keh (2013) for various values of the parameters k^*, k_w^*, η^*, a/b, and $d/(b-a)$. Analogous to the results of the current work, this mobility also decreases with an increase in k_w^*, a/b, and $d/(b-a)$, in general increases with increasing η^*, increases (decreases) with an increase in k^* for the case of $k_w^* < 1$ ($k_w^* > 1$), and is independent of k^* for the case of $k_w^* = 1$. However, the boundary effect on the thermocapillary motion of a fluid sphere in general is slightly stronger for this axially symmetric migration. For the general problem of a drop undergoing thermocapillary migration in an arbitrary direction within a cavity, the solution can be obtained by the superposition of both the axisymmetric and transverse results.

Acknowledgment

This research was partly supported by the National Science Council of the Republic of China.

References

Anderson, J. L. (1985): Droplet interactions in thermocapillary motion. *Int. J. Multiphase Flow*, vol. 11, pp. 813-824.

Barton, K. D.; Subramanian, R. S. (1990): Thermocapillary migration of a liquid drop normal to a plane surface. *J. Colloid Interface Sci.*, vol. 137, pp. 170-182.

Chang, Y. C.; Keh, H. J. (2006): Thermocapillary motion of a fluid droplet perpendicular to two plane walls. *Chem. Eng. Sci.*, vol. 61, pp. 5221-5235.

Chen, J.; Dagan, Z.; Maldarelli, C. (1991): The axisymmetric thermocapillary motion of a fluid particle in a tube. *J. Fluid Mech.*, vol. 233, pp. 405-437.

Chen, S. H.; Keh, H. J. (1990): Thermocapillary motion of a fluid droplet normal

to a plane surface. *J. Colloid Interface Sci.*, vol. 137, pp. 550-562.

Kasumi, H.; Solomentsev, Y. E.; Guelcher, S. A.; Anderson, J. L.; Sides, P. J. (2000): Thermocapillary flow and aggregation of bubbles on a solid wall. *J. Colloid Interface Sci.*, vol. 232, pp. 111-120.

Katz, E.; Haj, M.; Leshansky, A. M.; Nepomnyashchy, A. (2012): Thermocapillary motion of a slender viscous droplet in a channel. *Phys. Fluids*, vol. 24, pp. 022102-1-11.

Keh, H. J.; Chang, Y. C. (2010): Slow motion of a general axisymmetric slip particle along its axis of revolution and normal to one or two plane walls. *CMES: Computer Modeling in Engineering & Sciences*, vol. 62, no. 3, pp. 225-253.

Keh, H. J.; Chen, L. S. (1993): Droplet interactions in thermocapillary migration. *Chem. Eng. Sci.*, vol. 48, pp. 3565-3582.

Keh, H. J.; Chen, P. Y.; Chen, L. S. (2002): Thermocapillary motion of a fluid droplet parallel to two plane walls. *Int. J. Multiphase Flow*, vol. 28, pp. 1149-1175.

Lee, T. C.; Keh, H. J. (2012): Creeping motion of a fluid drop inside a spherical cavity. *Eur. J. Mech. B/Fluids*, vol. 34, pp. 97-104.

Lee, T. C.; Keh, H. J. (2013): Axisymmetric thermocapillary migration of a fluid sphere in a spherical cavity. *Int. J. Heat Mass Transfer*, vol. 62, pp. 772-781.

Loewenberg, M.; Davis, R. H. (1993): Near-contact, thermocapillary migration of a nonconducting, viscous drop normal to a planar interface. *J. Colloid Interface Sci.*, vol. 160, pp. 265-274.

Meyyappan, M.; Subramanian, R. S. (1987): Thermocapillary migration of a gas bubble in an arbitrary direction with respect to a plane surface. *J. Colloid Interface Sci.*, vol. 115, pp. 206-219.

Meyyappan, M.; Wilcox, W. R.; Subramanian, R. S. (1981): Thermocapillary migration of a bubble normal to a plane surface. *J. Colloid Interface Sci.*, vol. 83, pp. 199-208.

Nguyen, H.-B.; Chen, J.-C. (2011): Effect of slippage on the thermocapillary migration of a small droplet. *Biomicrofluidics*, vol. 6, pp. 012809-1-13.

Selva, B.; Cantat, I.; Jullien, M.-C. (2011): Temperature-induced migration of a bubble in a soft microcavity. *Phys. Fluids*, vol. 23, pp. 052002-1-12.

Subramanian, R. S.; Balasubramaniam, R. (2001): *The motion of bubbles and drops in reduced gravity* Cambridge University Press, Cambridge, UK.

Wan, Y. W.; Keh, H. J. (2011): Slow rotation of an axially symmetric particle about its axis of revolution normal to one or two plane walls. *CMES: Computer Modeling in Engineering & Sciences*, vol. 74, no. 2, pp. 109-137.

Yin Z.; Chang L.; Hu W.; Gao, P. (2011): Thermocapillary migration and interaction of two nondeformable drops. *Appl. Math. Mech.*, vol. 32, pp. 811–824.

Young, N. O.; Goldstein, J. S.; Block, M. J. (1959): The motion of bubbles in a vertical temperature gradient. *J. Fluid Mech.*, vol. 6, pp. 350-356.

Appendix A: Definitions of some functions in Section 2

$$\delta_n^{(1)}(\rho,z) = nr_2^{n-1}\frac{\partial r_2}{\partial r_1}P_n^1(\cos\theta_2) - r_2^n\frac{\mathrm{d}P_n^1(\cos\theta_2)}{\mathrm{d}\cos\theta_2}\sin\theta_2\frac{\partial\theta_2}{\partial r_1}, \tag{A1}$$

$$\delta_n^{(2)}(\rho,z) = -(n+1)r_1^{-n-2}\frac{\partial r_1}{\partial r_2}P_n^1(\cos\theta_1) - r_1^{-n-1}\frac{\mathrm{d}P_n^1(\cos\theta_1)}{\mathrm{d}\cos\theta_1}\sin\theta_1\frac{\partial\theta_1}{\partial r_2}, \tag{A2}$$

$$\delta_n^{(3)}(r,\theta) = -r^{-n-2}\frac{\mathrm{d}P_n^1(\cos\theta)}{\mathrm{d}\cos\theta}\sin\theta, \tag{A3}$$

$$\delta_n^{(4)}(\rho,z) = r_1^{-1}[nr_2^{n-1}\frac{\partial r_2}{\partial\theta_1}P_n^1(\cos\theta_2) - r_2^n\frac{\mathrm{d}P_n^1(\cos\theta_2)}{\mathrm{d}\cos\theta_2}\sin\theta_2\frac{\partial\theta_2}{\partial\theta_1}], \tag{A4}$$

$$\delta_n^{(5)}(r,\theta) = -r^{-n-2}P_n^1(\cos\theta)\csc\theta, \tag{A5}$$

$$\delta_n^{(6)}(\rho,z) = -r_1^{-1}r_2^nP_n^1(\cos\theta_2)\csc\theta_1, \tag{A6}$$

where

$$r_1 = [\rho^2+(z-d)^2]^{1/2}, \quad \cos\theta_1 = \frac{z-d}{r_1}, \quad \sin\theta_1 = \frac{\rho}{r_1}, \tag{A7}$$

$$r_2 = (\rho^2+z^2)^{1/2}, \quad \cos\theta_2 = \frac{z}{r_2}, \quad \sin\theta_2 = \frac{\rho}{r_2}; \tag{A8}$$

$$\frac{\partial r_2}{\partial r_1} = \frac{r_1+d\cos\theta_1}{r_2}, \quad \frac{\partial\theta_2}{\partial r_1} = r_2^{-2}[\frac{\partial r_2}{\partial r_1}(r_1\cos\theta_1+d) - r_2\cos\theta_1]\csc\theta_2, \tag{A9}$$

$$\frac{\partial r_1}{\partial r_2} = \frac{r_2-d\cos\theta_2}{r_1}, \quad \frac{\partial\theta_1}{\partial r_2} = r_1^{-2}[\frac{\partial r_1}{\partial r_2}(r_2\cos\theta_2-d) - r_1\cos\theta_2]\csc\theta_1, \tag{A10}$$

$$\frac{\partial r_2}{\partial\theta_1} = \frac{-r_1d\sin\theta_1}{r_2}, \quad \frac{\partial\theta_2}{\partial\theta_1} = r_2^{-2}[\frac{\partial r_2}{\partial\theta_1}(r_1\cos\theta_1+d) + r_1r_2\sin\theta_1]\csc\theta_2. \tag{A11}$$